SHRINKAGE BEHAVIOUR OF FCC CATALYST DROPLETS IN A SPRAY DRYING PROCESS

Stefan C.T. van der Sanden, W. Jan Coumans and Piet J.A.M. Kerkhof

Eindhoven University of Technology, Laboratory of Separation Processes and Transport Phenomena, P.O.Box 513, 5600 MB Eindhoven, The Netherlands.
Tel: +31-40-247-2359
Fax: +31-40-243-9303
E-mail: S.C.T.van.der.Sanden@tue.nl

Keywords: spray drying, drying conditions, shrinkage, crust formation, bulk density and porosity.

ABSTRACT

FCC catalyst is spray dried at several nozzle pressures and air inlet temperatures. The following physical properties of the obtained powder are measured: water content, mean particle size and particle size distribution, tapped bulk density and pore volume. All the investigated properties are directly related to the initial droplet size (distribution) and the shrinkage behaviour and crust formation of the droplet during drying. Next to the final particle size distribution, shrinkage also determines directly the porosity of the particle and hence the particle density. The bulk density depends on the particle density and is often influenced by the particle size distribution. In a part of this research the nozzle system and the physical properties of the feed have been kept constant. Results show that higher drying temperatures lead to an increase of the porosity. The bulk density decreases with higher drying temperatures. So it is likely that the mean particle size increases with increasing drying temperatures, although this was not measured. A theoretical model predicts a very rapid crust formation, during which shrinkage only occurs for a few percent. The experimental data show a volume shrinkage of about 90%, and so it is plausible that the crust remains deformable. This phenomenon can have large consequences for calculations of drying rates in spray drying of FCC catalyst.

INTRODUCTION

Spray drying is a widely used process to produce powders from a liquid feed containing dissolved and/or suspended solids. The drying of atomised droplets in the process involves simultaneous mass, heat

and momentum transfer. The variety of the nature of spray dried materials is so large that each material has its own characteristic drying behaviour and product properties. When the feed is a slurry, the formation of a crust is supposed to occur almost instantaneously. The crust could have a considerable influence on the drying kinetics, caused by increased resistance to heat and mass transfer [Audu (1975), Cheong (1986)]. The nature of the crust is of great importance for the crust structure, porosity and strength. Fluid Catalytic Cracking (FCC) catalyst is a porous powder consisting of zeolite Y and clay, binded together in a silica-alumina matrix. FCC catalyst is considered as particles having a solid structure made of inert particles with a diameter in the order magnitude of 1 μm. The porosity is defined as voids present between these particles. Literature on spray drying of catalytic materials is rare [Lebeis (1955), Pedersen (1989), Andrieu (1992), Woltermann (1993)], however several publications exist concerning the spray drying of slurries and the influence of spray drying conditions on product properties [e.g. Duffie (1953), Crosby (1958), Charlesworth (1960), Meenan (1997)]. Miura *et al.* [Miura (1972)] found that the drying rate of a single droplet of suspended bentonite was equal to the drying rate of pure water and observed no crust formation in the drying process for all initial water contents and drying temperatures. Schlünder analysed the observation that that partially wetted surfaces can extend the constant rate period [Schlünder (1988)]. Audu *et al.* [Audu (1975), Cheong (1986)] introduced a model that incorporates crust formation and thickening during drying and concluded that the crust is the major resistance to mass transfer. In the model the crust does not shrink and has an outer diameter equal to the initial droplet diameter.

In this paper we consider the influence of drying conditions on the mean particle size, bulk density and porosity of FCC catalyst. These properties are directly related to the shrinkage behaviour and crust formation of the feed droplets in the spray drying process. It is not our goal to present a drying model for FCC catalyst, but to show the possible influence of drying conditions on crust formation and the effects on final particle properties.

THEORY AND MODELLING

Shrinkage model

A shrinkage model has been derived that relates the relative final particle diameter, the particle porosity and the bulk density to the amount of shrinkage. The model enables calculation of the amount of shrinkage from the measured particle porosity. Also the initial droplet diameter and the bed porosity can be calculated from the measured particle porosity. In the model it has been assumed that:

- the droplet is spherical and shrinks uniformly.
- the components of the FCC catalyst are one (monosized) solid phase without internal porosity. There is no physical or chemical interaction between the components themselves and between the liquid phase and the solid phase. Thus the densities of the solid phase, d_s, and of the liquid phase, d_w, are constant.
- there is no vapour phase present in the droplet. When the droplet stops shrinking, the volume of the water present at that time is equal to the volume of the pores after drying.

Definitions:

The particle properties have been calculated with the densities of the solid, d_s, and the liquid phase, d_w, together with the initial water content of the feed, X_0. The shrinkage-coefficient, S, has been defined as the ratio of the actual amount of volume decrease to the maximum possible volume decrease:

$$S = \frac{V_0 - V_p}{V_0 - V_s} \tag{1}$$

The density of the feed is given by:

$$\rho_0 = \frac{1 + X_0}{\frac{1}{d_s} + \frac{X_0}{d_w}}, \tag{2}$$

in which the density of the solid phase is equal to the mass averaged density of the components:

$$d_s = \sum_{j=1}^{n} \omega_j \cdot d_j \tag{3}$$

Particle properties:

The shrinkage-coefficient has been calculated with the measured particle porosity via:

$$S = 1 - \frac{\varepsilon_p}{1 - \varepsilon_p} \cdot \frac{d_w}{d_s} \cdot \frac{1}{X_0} \tag{4}$$

The initial droplet diameter has been calculated with the particle porosity and final particle diameter:

$$2R_0 = 2R_p \cdot \left[\left(1 - \varepsilon_p\right) \cdot \left(1 + \frac{d_s}{d_w} X_0 \right) \right]^{1/3} \tag{5}$$

The bed porosity has been calculated with the measured bulk density and particle porosity:

$$\varepsilon_{bed} = 1 - \frac{\rho_{bed}}{d_s (1 - \varepsilon_p)} \tag{6}$$

Numerical drying model

The drying kinetics has been described with a diffusion model [e.g. Kerkhof (1975), Van der Lijn (1976)]. The drying conditions determine the development of the concentration profiles inside the droplet and thereby the concentration at the surface. It is assumed that the droplet forms a crust when the surface reaches a water concentration of 21 wt.%. This stage we denote as the initial crust formation stage. With the shrinkage model the particle porosity and bulk density at the end of this stage have been calculated.

The spray drying process has been assumed to be ideally mixed and droplets had no internal gas phase present. The diffusion equation reads:

$$\frac{\partial \rho_w}{\partial t} = \frac{1}{r^2} \frac{\partial}{\partial r} \left(r^2 D_{ws} \frac{\partial \rho_w}{\partial r} \right) \tag{7}$$

with initial and (moving) boundary conditions:

$$\begin{aligned} t = 0 \quad & 0 \le r \le R \quad && \rho_w = \rho_{w,0} \\ t > 0 \quad & r = 0 && \frac{\partial \rho_w}{\partial r} = 0 \\ & r = R(t) && J_{w,i} = k_f \left(\rho_{v,i} - \rho_{v,b} \right) \end{aligned} \tag{7a,b,c}$$

The co-ordinates have been transformed to water-free solid co-ordinates. A flat temperature profile has been assumed for the droplet:

$$\rho_l c_{p,l} \frac{dT}{dt} = \frac{3}{R(t)} \left(\alpha \left(T_b - T_p \right) - J_{w,i} \left(c_{p,v} T_p + \Delta H \right) \right) \tag{8}$$

It has been assumed that diffusion can be described as Brownian motion and the binary diffusion coefficient has been calculated with the Stokes-Einstein equation:

$$D_{ws} = \frac{k_B T}{3 \pi \eta_w \delta_s} \tag{9}$$

EXPERIMENTAL

The spray drier

In this research a pilot plant scale co-current spray drier by Niro Atomizer has been used. The air enters the drying chamber via an annulus, and the atomiser is placed in its centre. The air exits the drier via a downwarded pipe, which is placed in the centre of the chamber. The diameter of the drying chamber is 2.20 m and the total height is 3.70 m with a conical angle of 60° at 2.0 m from the top. The feed is atomised by a pressure nozzle (Spraying Systems SK), producing a hollow conical spray with a spray angle of 80°. Product was both collected from the drying chamber (tower product) and the cyclone (cyclone product).

FCC catalyst formulation and preparation

The catalyst formulation used in this work was a mixture of 24 wt.% zeolite Y, 47 wt.% clay, 15 wt.% alumina and 14 wt.% silica. Dry solids contents were based on drying at 200 °C for 48 hours. A silica sol was prepared by mixing sodium silicate and sulphuric acid in a vessel at constant pH. Kaolin clay was added gradually to the sol. Subsequently zeolite Y and alumina were added. Finally the water content of the feed was circa 3.6 kg_w/kg_{ds} (solids content was circa 21.7 wt.%).

Characterisation

The water content of the product has been determined after 48 hours drying at 200 °C. The particle size distribution has been measured with laser scattering (Coulter LS-130). The skeletal density has been determined with a Helium stereopycnometer (Quantachrome). The bulk density has been measured using a Stampfvolumeter (Engelsmann) with a graduated cylinder of 250 ml. The total pore volume has been determined with incipient wetness impregnation of water [Leofanti (1998)]. The porosity was then calculated using the skeletal density.

RESULTS AND DISCUSSION

Spray drying experiments

Table 1. Process conditions of the experiments with constant feed-flow.

Experiment	Number	*1*	*2*	*3*	*4*
Air flow	[kg_{da}/s]	0.183	0.176	0.174	0.156
Air inlet humidity	[g_w/kg_{da}]	7.60	5.39	6.55	6.85
Air inlet temperature	[° C]	302	331	363	393
Feed-flow	[kg/s]	40.2	40.2	40.2	40.2
Initial water content	[kg_w/kg_{ds}]	3.61	3.61	3.59	3.72
Feed temperature	[° C]	22.8	22.5	22.9	22.6
Nozzle pressure	[bar]	17.8	18.9	17.1	15.9
Air outlet humidity	[g_w/kg_{da}]	55.4	55.1	56.7	63.3
Air outlet temperature	[° C]	131	149	156	176

In figure 1 the measured mean particle diameter and the calculated mean initial droplet diameter have been plotted as function of the nozzle pressure for all experiments. The mean particle diameter was mainly determined by the nozzle pressure and correlated to the nozzle pressure by the power of -0.26, which is somewhat less than known from literature [e.g. Trullinger (1997), Masters (1985)]. Figure 2

shows the influence of the drying conditions on the mean particle diameter at constant feed-flow. A higher drying rate does not influence the particle size of the product mix. The increase of the mean

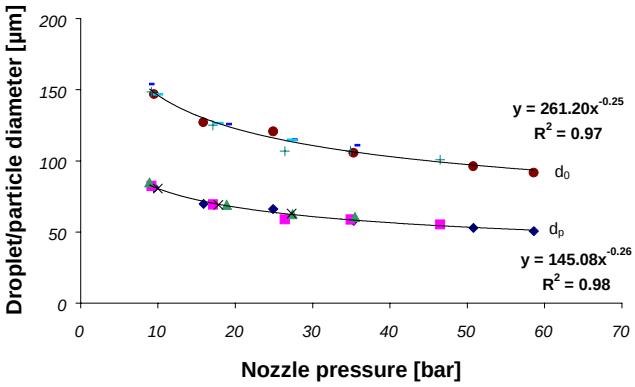

Figure 1: Average particle/droplet diameter as function of nozzle pressure.

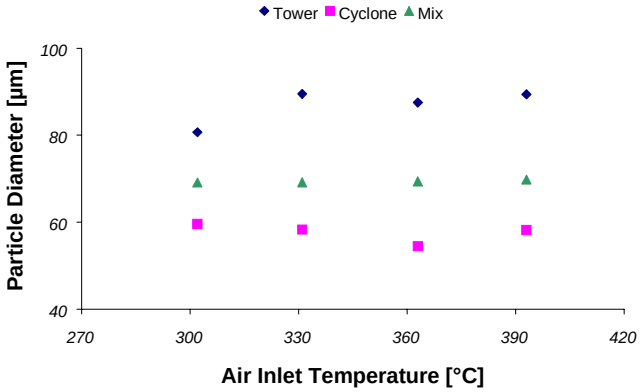

Figure 2: Average particle diameter as function of air inlet temperature.

particle diameter of the tower product and the decrease of mean particle diameter of the cyclone product could not be explained by changes in tower to cyclone product-ratio. The variance of the particle size distribution was roughly the same for tower and cyclone product and increased slightly with increasing drying temperatures. In figure 3 it is shown that the porosity increased somewhat with increasing drying rates. Also it can be seen that the tower product had a slightly higher porosity. As expected from the porosity data, the bulk density decreased with increasing drying temperatures (figure 4). The bulk density of the cyclone product was somewhat higher than of the tower product. This is probably more due to lower particle porosity than a lower bed porosity, as the variance of the particle size distribution for the tower product and cyclone product was the same.

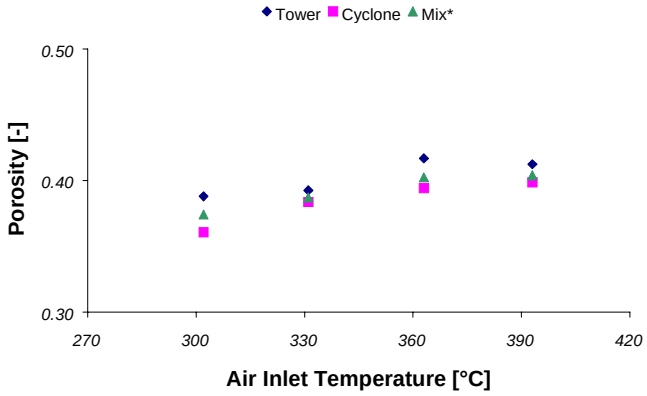

Figure 3: Particle porosity as function of air inlet temperature

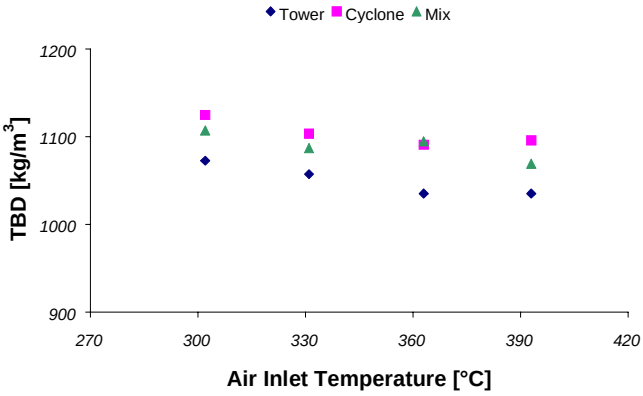

Figure 4: Tapped bulk density as function of air inlet temperature

Shrinkage model

The shrinkage model calculates the relative particle diameter, the particle porosity and the bulk density (calculated with a bed porosity of 0.3) as function of the shrinkage-coefficient (figure 5). It can be seen that the influence of the shrinkage-coefficient on particle properties is most distinct at high values of *S*, and small changes in particle size have considerable influence on porosity and bulk density. The shrinkage model enables calculation of the shrinkage-coefficient, the mean initial droplet size and the bed porosity from the measurements (results are listed in table 2). The shrinkage-coefficient decreased slightly with increasing drying temperatures. The influence of the drying rate on relative particle diameter and the bed porosity was less clear.

Table 2. Calculated data from measurements and the shrinkage model.

Experiment	Number	*1*	*2*	*3*	*4*
Shrinkage-coefficient	[-]	0.932	0.929	0.923	0.926
d_p/d_0	[-]	0.546	0.550	0.555	0.550
ε_{bed}	[-]	0.275	0.273	0.250	0.265

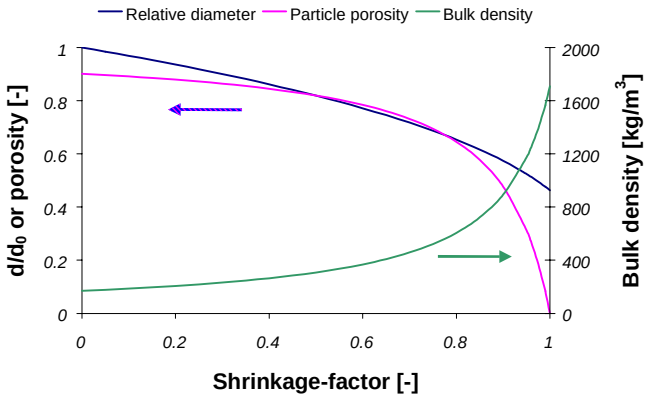

Figure 5: Relative particle diameter, porosity and bulk density as function of the shrinkage-factor

Numerical model

The numerical model enabled the calculation of water concentration profiles in the droplet as a function of the drying time for given process conditions. The end of the first crust formation stage was taken when the water concentration at the surface reached a certain value, ω_w = 21 wt.%.

Table 3. Calculated shrinkage-coefficients and relative particle diameters from the numerical model.

Experiment	Number	*1*	*2*	*3*	*4*
S	[-]	0.0178	0.0143	0.0125	0.0110
d_p/d_0	[-]	0.9946	0.9957	0.9962	0.9967
ε_p	[-]	0.899	0.900	0.900	0.900
Bulk density	[kg/m^3]	172.0	171.4	171.1	170.9

The predicted initial shrinkage-coefficients were very small, indicating that the particle forms a crust in a very early stage of the drying process. The initial shrinkage-coefficient decreased slightly with increasing air temperature. The calculated particle porosity and bulk density at initial crust formation deviated much from the measured final porosity and bulk density, also indicating that shrinkage also occurs after formation of a crust.

CONCLUSIONS

The properties of FCC catalyst, considered in this paper, are not much influenced by spray drying conditions. The mean particle size and size distribution are mainly determined by the nozzle type and the applied pressure. The shrinkage model shows a large influence of the amount of shrinkage on the particle porosity and bulk density at high shrinkage-coefficients. The shrinkage model and the measured properties of spray dried FCC catalyst indicate that the droplets almost shrink to a maximum amount. Although the influence of the drying conditions is very limited, the droplets shrink less when dried at higher air temperatures. This could be due to shorter drying times, which result in a more random packing of the components, causing a higher porosity. Consequently the bulk density decreases with increasing drying temperatures.

The numerical model predicts a high concentration of solids at the surface in an early stage of the drying process under the experimental spray drying conditions. This strongly indicates that a crust is formed in an early stage of the drying process. However, when a crust has been formed and the droplet keeps shrinking the crust has to remain deformable during the drying process.

The presence of a crust will influence the drying kinetics of the FCC catalyst, although it is not yet clear if the crust will lower the drying rate or that the wetting of the surface is large enough to maintain the constant drying rate.

NOTATION

Roman symbols:		
c_p	heat capacity	kJ/kg K
d	true density	kg/m^3
D	diffusion coefficient	m^2/s
ΔH	latent heat of vaporisation	kJ/kg
J	mass flux	kg/m^2 s
k	external mass transfer coefficient	m/s
k_B	Boltzmann constant	$1.38 \cdot 10^{-23}$ J/K
r	radius	m
R	outer radius	m
S	shrinkage-coefficient	m^3/m^3
t	time	s
T	temperature	° C
V	volume	m^3
X	water content	kg_w/kg_s
Greek Symbols		
α	external heat transfer coefficient	W/m^2 s
δ	component diameter	m
ε	porosity	m^3/m^3
η	viscosity	Pa s
ρ	volumetric concentration/density	kg/m^3
ω	mass fraction	kg_i/kg_{tot}
Subscripts		
0	initial condition	
b	bulk	
bed	bed	
f	film-layer	
i	interface	
ln	logarithmic mean	
p	particle	
s	solid	
v	water vapour	
w	liquid water	

LITERATURE

Andrieu, J., Dessalces, G., Joly-Vuillemin, C., Reymond, J.P., Kolenda, F., Spray Drying as a Shaping Technique for Catalyst Production, in: Drying '92, 1992, 533-542.

Audu, T.O.K., Jeffreys, G.V., 1975, The Drying of Drops of Particulate Slurries, Transactions of the Institution of Chemical Engineers, 53, 165-172.

Charlesworth, D.H., Marshall, W.R., Jr., 1960, Evaporation from Drops Containing Dissolved Solids, American Institute of Chemical Engineers Journal, 6 (1), 9-23.

Cheong, H.W., Jeffreys, G.V., Mumford,C.J., 1986, A Receding Interface Model for the Drying of Slurry Droplets, American Institute of Chemical Engineers Journal, 32 (8), 1334-1346.

Crosby, E.J., Marshall, W.R., Jr., 1958, Effects of Drying Conditions on the Properties of Spray-dried Particles, Chemical Engineering Progress, 54 (7), 56-63.

Duffie, J.A., Marshall,W.R.,Jr., 1953, Factors Influencing the Properties of Spray-dried Materials, Chemical Engineering Progress, 49 (8), 417.

Kerkhof, P.J.A.M., 1975, A Quantative Study of the Effect of Process Variables on the Retention of Volatile Trace Components in Drying, Ph.D. Thesis, Technische Universiteit Eindhoven, Eindhoven.

Lebeis, E.H., Burtis, T.A., 1955, Effect of Drying Conditions on Drying Rate and Physical Properties of a Porous Solid, American Institute of Chemical Engineers Journal, 1 (3), 329-334.

Leofanti, G., Padovan, M., Tozzola, G., Venturelli, B., 1998, Surface Area and Pore Texture of Catalysts, Catalysis Today, 41, 207-219.

Van der Lijn, J., 1976, The "Constant Rate Period" during the Drying of Shrinking Spheres, Chemical Engineering Science, 31, 929-935.

Masters, K., 1985, Spray Drying Handbook, Longman Scientific & Technical, Essex, England.

Meenan, P., Roberts, K.J., Knight, P.C., Yuregir, K., 1997, The Influence of Spray Drying Conditions on the Particle Properties of Recrystallized Burkeite, Powder Technology, 90, 125-130.

Miura, K., Atarashiya, K., Ouchi, I., Ohtani, S., 1972,Experimental Study of Drying Characteristics of Single Drops Containing Solids, Heat Transfer-Japanese Research, 1 (2), 11-17.

Pedersen, L.A., Lowe, J.A., Matocha, C.K., Sr., 1989, Attrition- and Metal-resistant Fluid Cracking Catalyst Prepared with Alumina Powder in the Matrix, in: Characterization and Catalyst Development: an Interactive Approach, editors: Bradley, S.A., Gattuso, M.J., Bertolacini, R.J., ACS Symposium Series No.411, Chapter 38, 414-429, Washington DC., USA.

Schlünder, E-U., 1988, On the Mechanism of the Constant Drying Rate Period and its Relevance to Diffusion Controlled Catalytic Gas Phase reactions, Chemical Engineering Science, 43 (10), 2685-2688.

Trullinger, C., 1997, Controlling Atomization in your Spray Dryer, Powder and Bulk Engineering, April, 87-94.

Woltermann, G.M., Magee, J.S., Griffith, S.D., 1993, Commercial Preparation and Characterization of FCC Catalysts, in: Fluid Catalytic Cracking: Science and Technology, Editors: Magee, J.S., Mitchell, M.M.Jr., Elsevier, Amsterdam.